View metadata, citation and similar papers at core.ac.uk
brought to you by CORE
provided by Digital.CSIC

Influence of charcoal fines on the thermoplastic properties of coking coals and the optical properties of the semicoke

Adrià Guerrero, María A. Diez, Angeles G. Borrego*

Instituto Nacional del Carbón (INCAR-CSIC), c/ Francisco Pintado Fe 26, 33011 Oviedo, Spain.

*Corresponding Author: Tel.:+34985119090; Fax: +34985297662

e-mail address: angeles@incar.csic.es

Abstract

The aim of this work is to investigate the influence of the addition of organic inerts such as charcoal with a well-controlled particle size on the development of fluidity in three coking coals of different rank, maceral composition, and rheological properties. Three size fractions of charcoal, <20, 20-80, and 80-212 μm, that can be considered as artificially prepared inertinites were used. The different charcoal fractions were added in amounts of 2, 5, 10, and 15 wt% to selected high-quality coking coals with a Gieseler maximum fluidity (Fmax) of 373 (LF), 541 (MF), and 1891 (HF) ddpm. Increasing the amount of charcoal in the blend led to a progressive inverse exponential reduction in fluidity. This reduction was accompanied by a shortening of the fluid interval due to an increase in the softening temperature. In the case of the finest charcoal fraction, the inhibition of fluidity was even more pronounced. The HF coal with a relatively high fluidity was very sensitive to minimum amounts of charcoal addition, losing nearly half of its fluidity when 5 wt% charcoal was added. A similar reduction in Fmax was also observed for LF, while MF with only a slightly higher fluidity displayed a different trend. From the results it can be seen that the inherent characteristics of a coal are critical factors that affect the extent of the

reduction in fluidity caused by the incorporation of charcoal. The differences can be partially attributed to the amount of inertinite present in the parent coal and to the macerals within the inertinite, especially fusinite, semifusinite, and inertodetrinite. In relation to petrographic changes in the matrix of the semicokes, there is a general trend for isotropic material to increase and the size of the anisotropic textures to decrease with the addition of charcoal. Inclusions within the semicoke matrix also change according to the amount and the size of the charcoal added to coal.

Keywords: Coking coal, charcoal, inertinite, fluidity, semicoke, optical texture

1. Introduction

Coals used for the production of metallurgical coke have certain physical properties which cause the individual coal particles to soften, liquefy, agglomerate and, then, resolidify into a hard and porous carbon material (semicoke) when heated up to 500 ºC in an oxygen-deficient atmosphere. With further heating up to 1000-1200 ºC, this intermediate carbon material is converted into a high-temperature coke with a strong mechanical resistance and moderate reactivity towards CO_2. The development of fluidity up to 500 ºC is considered a key step in coal thermochemical behaviour in a coke oven and, consequently, for the structure and properties of the resultant coke (Patrick, 1975; Loison et al., 1989; Marsh, 1992; Butterfield and Thomas, 1995; Diez, 2014). In fact, the optical texture achieved in the semicoke stage is generally retained in the coke (Patrick et al., 1973; 1979; Fukuyama et al., 1981; Fortin and Rouzaud, 1993; 1994).

Any pre-treatment of coal or incorporation of carbon-containing additives that alter the physical and chemical processes will modify the development of coal fluidity (Clemens and Matheson, 1995; Sakurovs, 2000; Fernandez et al., 2009). Chemically active additives such as pitch, tar, petroleum residues, polymers, and oils may act as fluidity enhancers or inhibitors depending on their ability to donate and/or accept transferable hydrogen, whereas inert additives (anthracite, char, breeze coke, calcinated coke, oxygenated polymers) have a detrimental effect on fluidity (Valia and Hooper, 1994; Menendez et al., 1996; Barriocanal et al., 1998; Diez et al., 2005; Diez et al. 2012a). This detrimental effect has been attributed to the presence of oxygen-rich volatiles, the greater surface area of the additives that adsorbs some of the tar contributing to plasticity, or to the smaller particle size of the additives. Thus, among the factors affecting fluidity when carbonaceous additives in a solid state are added are not only the amount of additive, but also the type and size (Loison et al., 1989; Sakurovs 2000; Diez et al., 2009).

In recent years, the incorporation of woody biomass such as charcoal in coal blends for cokemaking has attracted a great deal of interest as a way to reduce fossil CO_2 emissions (Hanrot et al., 2009; MacPhee et al., 2009; Ueda et al., 2009; Pohlmann et al., 2010). The processes involved in the formation of charcoal to a certain extent resemble those of the formation of inertinite in coal (Diessel, 1992). There are, however, striking differences such as the fact that the charcoal is not subjected to coalification and that artificial charcoals can be expected to show less variability than those formed in nature during forest fires (Scott and Glasspool, 2007) or after extensive oxidation processes in cold-temperate peatlands (Taylor et al., 1989). Studies performed over the years on the behavior of inertinite during the coking process and on its influence on coke properties have shown that: i) a significant part of inertinite is transformed during the process, with the most reactive inertinite developing an anisotropic mosaic optical texture while the least reactive inertinite remains isotropic (Taylor et al., 1967; Diessel, 1983; Diessel and Wolff-Fischer, 1986); ii) the assumption that only one third of the semifusinite in Carboniferous coals reacts, which has been commonly held for years when formulating coal blends (Ammossov et al., 1957, Schapiro et al., 1961), underestimates the amount of reactive inertinite in Gondwana and many younger coals (Pearson and Price, 1985; Diessel and Wolff-Fischer, 1986; Gransden et al., 1991; Choudhury et al., 2008); iii) the fusibility of inertinite is strongly and inversely related to its reflectance (Diessel, 1983; Diessel and Wolf-Fischer, 1987; Komorek and Morga, 2007, Pusz et al., 2009; Guerrero et al., 2013); iv) small inertinite components such as micrinite or inertodetrinite, regardless of their poor fusibility, may have a positive effect on coke strength because they are easily integrated within the coke matrix (Mackowsky 1977); and v) large particles (over 50 microns), on the contrary, favour the propagation of fissures and cause a decrease in mechanical strength (Miyazu, 1974). The

addition of charcoal to coal would, therefore, act as an inert carbon additive and reduce fluidity (Sakurovs, 2000; Diez et al., 2012a; 2012b; Montiano et al., 2013). The level of reduction has been shown to be dependent on the amount (Ng et al., 2012), and type (Diez and Borrego, 2013) of charcoal added, the severity of the pre-treatment to which it has been subjected, and its size (Sakurovs, 2000; MacPhee et al., 2009). This work attempts to study the effect of the addition of well-controlled size fractions of charcoal to coals of different fluidity, rank, and petrographic composition. The difference between this and other previous works in which charcoals of different sizes have been added (MacPhee et al., 2009) is essentially the smaller size of the charcoal used in the present study, corresponding to a size-range typical of organic inerts in coal (inertinite macerals). Special attention is paid to the differences between the parent inertinite and the added charcoal, the effect of the additions on fluidity and on the optical texture of the semicoke, and also to the way in which the charcoal is incorporated into the semicoke matrix.

2. Experimental

Three coals from the United States and Australia, which are typically used in formulation of metallurgical coal blends, were selected. The series comprised coals of different fluidity and will be referred to as lower, medium, and higher fluidity coal (LF, MF, and HF, respectively). The charcoal is a commercial charcoal originating from Brazil which is used for metallurgical purposes and is produced at a nominal temperature of 450 ºC. The chemical characterization of the coals and charcoal (CH) consisted of a proximate (ISO 17246:2010) and ultimate analysis (ISO 29541:2010 for C, H, and N content and ISO 19579:2006 for total sulfur content). The thermoplastic characteristics of the coals and the coal-charcoal blends were determined by using a constant-torque Gieseler plastometer (ASTM D2639). Briefly, the samples (5 g, <0.425 mm)

were heated from 300 ºC up to 500 ºC at a heating rate of 3 ºC/min, the rotation of a stirrer placed inside the sample indicating the fluidity, which was recorded in dial divisions per minute (ddpm), as a function of the temperature. The maximum fluidity value (Fmax), and the temperatures of maximum fluidity (Tf), softening (Ts), and resolidification (Tr) were also recorded. The plastic or fluid interval was defined as the difference between Tr and Ts. The Gieseler semicokes were recovered for a petrographic analysis of the optical texture. The petrographic analysis of the coal consisted of performing a combined maceral-reflectance analysis, recording the reflectance of every maceral selected by point-counting. The relevant standards were ISO 7404-05:2009 for measuring the maceral reflectance and ISO 7404-03:2009 for choosing the components. For each coal, 500 reflectance values were recorded and assigned to the corresponding maceral and/or maceral group, allowing detailed information on the maceral compositions and their reflectance distributions to be collected. The nomenclature used was that of the International Committee for Coal and Organic Petrology (ICCP, 1998; 2000). Identification of the inertinite and liptinite macerals was performed at maceral level. However, the liptinite is reported at the maceral-group level due to the small amount of this component and the fact that most of it consisted of sporinite. Identification of vitrinite components was performed at maceral subgroup level, distinguishing between components derived from tissues that maintain their integrity (telovitrinite), vitrinite that acts as a matrix for other components (detrovitrinite), and pure gelified material (gelovitrinite).

The charcoal size fractions were separated by wet-sieving from a sample ground to a top size of 212 μm using a succession of sieves of different sizes and finally a collection flask for the smallest fraction (Fig. 1). The charcoal water-slurry with particles below 20 μm was then filtered

under vacuum using a Millipore glass fiber filter. The fractions selected were: 212-80 µm (CH212), 80-20 µm (CH80), and <20 µm (CH20). The suitability of the CH fractions was assessed by Coulter analyses using ethanol as dispersant and by scanning electron microscopy (SEM). The coals were blended with each charcoal fraction in amounts of 2, 5, 10, and 15 wt% to yield a total of 36 coal-charcoal samples (12 for each coal).

The optical texture of the 36 Gieseler semicokes was determined using the classification of the ASTM D5061-07 standard plus some additional categories for the discrimination of coal and charcoal inerts. The components of the semicokes were divided into the following categories: a) a matrix comprising isotropic and anisotropic material with a mosaic, lenticular, or fiber texture; b) organic inert inclusions comprising components with smooth edges probably derived from inertinite present in the coal and components with sharp edges of different size probably derived from the added charcoal; and c) mineral matter (Gray and Devanney, 1986).

As the coal-charcoal blends were prepared by weight and identification of the charcoal in the semicokes can only be performed on a volume basis, the real densities of the coal, charcoal, and coal minerals ashed at below 500 ºC were measured to perform the weight-to-volume conversions so that a relationship could be established between i) the amount of inertinite in the coal and that identified in the semicokes and ii) the amount of added charcoal and its amount identified in the semicoke. The real density of the different components was determined by He picnometry. Prior to analysis the samples were outgassed under vacuum at 90ºC for 90 minutes. However, an additional calculation was required because of the loss of volatiles during the Gieseler assay. The Gieseler semicokes typically retain 10% of their volatiles regardless of the

rank of the parent coal (Loison et al., 1989; van Krevelen 1993). Although at the rank of coking coals the differences in volatile matter content of the various maceral groups are not very large, the coke yield of inertinite can be expected to be slightly higher than that of vitrinite. The expressions used for volatile loss of the maceral groups were those of Borrego et al. (2000), it being assumed that the semicoke retains 10% of its volatile matter content.

3. Results and Discussion

3.1 Coal and charcoal characteristics

The three bituminous coals are characterized by an ash content of below 10 wt% and a sulphur content of below 1 wt% (Table 1) as typically required for prime coking coals used for metallurgical coke production. They range in volatile matter content from 27.2 to 21.2 wt% daf and in vitrinite reflectance from 1.18 to 1.25 % (Table 2), both of these parameters moving in opposite directions. The comparatively low volatile matter content of the LF coal even though its vitrinite reflectance is only 0.03 % higher than that of MF is due to its larger inertinite content (22.2 vs 14.8 %, Table 2), which typically has less volatile matter than vitrinite (Borrego et al., 2000). Other rank chemical parameters vary as expected, with C increasing and H and O decreasing as vitrinite reflectance increases (Table 1). A general trend for the Gieseler maximum fluidity (Fmax) and plastic interval to decrease with increasing coal rank was observed. The difference in fluidity between MF (541 ddpm) and HF (1891 ddpm) is relatively large for two coals whose vitrinite reflectances only differ by 0.03%. The real density of the coal organic matter, calculated from the density values of the coals and the low-temperature-ashed mineral matter (2.73 g cm^{-3}), ranges between 1.20 and 1.24 g cm^{-3} and is similar for both MF and HF. These values are slightly lower than expected for coals with similar carbon contents (Gan et al.,

1972, and van Krevelen, 1993). Compared to the chemical compositions of the coals, the charcoal has a lower carbon and hydrogen content but a significantly higher oxygen content. The total sulfur and ash contents are very low, whereas the volatile matter content is within the range of that of the coals (Table 1). The differences in chemical composition of the charcoal and coals will affect the composition of the volatiles released upon carbonization (mainly oxygen-rich gases in the case of the charcoal and hydrogen and hydrocarbons in the case of coals). It should be noted that the helium density of the charcoal is higher than that of the organic matter in the coal (Table 1), which is consistent with the fact that the He density of inertinite is higher than that of vitrinite in coals (van Krevelen, 1993).

Petrographic characterization revealed further differences between the coals. The inertinite content ranges from 14.8 vol% in MF to 22.2 vol% in LF whereas the liptinite content is very low and consists mostly of sporinite (Table 2). Telovitrinite is by far the most abundant vitrinite subgroup and the reflectances of both subgroups (telovitrinite and detrovitrinite) are very similar, indicating a significant homogeneity of vitrinite optical properties within each coal. The most abundant inertinite maceral is semifusinite, which accounts for around 50% of the total inertinite content of the coals. The reflectance of fusinite is one of the highest, whilst semifusinite has one of the lowest reflectances within the inertinite group. The relative abundances of inertinite macerals in LF and HF are very similar, whereas MF has a higher inertodetrinite and a lower fusinite content than the others. The charcoal reflectance measured in the two largest fractions is 2.03%, which is slightly higher than the average value for inertinite in MF and HF and similar to the inertinite reflectance of LF. The scatter of reflectances in the charcoal is larger as a consequence of the inhomogeneity of the carbonization process. Although the average charcoal

reflectance is higher than the average inertinite reflectance of the coals, other statistics such as the mode (1.81%) and the median (1.78%), are close to the average reflectance of semifusinite, which is the main inertinite maceral in these coals (Table 2).

3.2 Morphology of the charcoal fractions

The morphology of the charcoal fractions used for blending is shown in Fig.2. The particles in CH212 and CH80 exhibit a cell-wall structure typical of oxidized or charred lignocellulosic tissues from woody plants (i.e. the appearance characteristic of fusinite in coal). However, the charcoal particles show no evidence of deformation or compaction, as is commonly observed in inertinite and particularly in semifusinite macerals. This feature would be useful for helping to distinguish charcoal particles from inertinite in the microscopic examination of semicokes. The particles in the largest fraction have a clear fusiform shape, with a width of < 212 μm, but a length that is significantly larger than that. The smaller particles are more equidimensional and the voids have almost disappeared in the particles of the smallest fraction, where only fragments of the cell walls remain, often with a “Y” or “X” shape. These particles, which have an average diameter of 12 μm, fall within the range of inertodetrinite in coal. The size distribution also shows that most of the particles in the finest fraction are distinguishable with an optical microscope, because the amount of particles below two microns size is very small. As the fine hydrophobic organic particles tend to group together when embedded in the mounting resin, a special effort to homogenize must be made when preparing the blends. The possibility of some of the particles segregating during the sieving process was taken into account and the consistency of size distribution within each fraction was also checked. Table 3 shows the ash contents, densities, and the size distributions of the different charcoal fractions. The density values

increase slightly with the increase in ash content from CH212 to CH20, reflecting a slight trend towards enrichment of the mineral matter due to its liberation during grinding. This is a very common phenomenon in coal, where the segregation is even greater than in the present case (Mendez et al., 2003). The density of the organic matter remains similar (Table 3) and the scatter of charcoal reflectances in the two largest fractions is also similar, indicating that segregation of organic components with different charring intensities has not occurred. The size distribution also shows very little overlapping for the most common sizes between the different fractions.

3.3. Influence of charcoal addition on coal fluidity development

Gieseler plasticity is an important test not only for evaluating the coking capacity of coals and the effect of either chemically and/or physically inert or active additives on a specific blend, but also for assessing the optimum amount of additive required for a particular blend (Diez and Alvarez, 2013). The interactions between coal and charcoal in the plastic stage of the carbonization process will be reflected in the variation of Gieseler parameters. Fig. 3 shows the variation of Fmax for the various blends with the addition of charcoal to the three coals in different amounts. In all cases, biomass addition causes a decrease in Fmax which shows an exponential trend. The shapes of the exponential curves are different and not exclusively related to the rank and/or fluidity of the parent coals. This finding suggests that the extent of reduction must be the result of a combination of both the type of coal and the particle size of the charcoal used. In general, these results are consistent with the view that the addition of any type of biomass to coking coals reduces their capacity to develop a fluid phase during thermal treatment (Diez et al., 2012a; Castro Diaz et al., 2012). The greater surface area of the fine inert particles is

at least partially responsible for binding the plasticising fraction of a coal and, consequently, favouring the inhibition of fluidity development (Loison et al., 1989).

The comparison of the general trends of the blends made up of the coking coals and charcoal reveals certain similarities and differences. For a charcoal addition of 2 wt%, the drop in Fmax of the HF blends shows only small differences depending on which of the biomasses is added, the reduction varying between 28-32%. When the amount of charcoal in the blend is increased to 15 wt%, the effect of charcoal particle size becomes more prominent. In the case of MF and LF coals significant differences in Fmax arise from the addition of charcoal of different sizes to the coal even in small amounts (2 wt%). The solid particles from charcoal are more easily embedded into the fluid system of the MF coal which experiences the smallest reduction in fluidity at all levels of addition and all three charcoal particle sizes. This trend is more clearly appreciated in Fig. 4 where the loss in fluidity expressed as a percentage of the original Fmax is plotted for the various coal-charcoal blends. With regard to the ability of the LF and HF coals to incorporate charcoal into their fluid mass, the reduction in Fmax is greater in HF than in LF for the addition of up to 5 wt% charcoal whereas the opposite occurs for 10-15 wt% additions. The highest losses in Fmax and the smallest differences between the blends are observed with high additions (10-15 wt%) of the finest charcoal (Fig. 4).

The reduction that an inert carbon material such as charcoal can cause is attributed to its high physical adsorption capacity. Charcoal can adsorb the decomposition products from coal which can then act as plasticizers so that they are responsible for any modification of softening and fluidity development (Loison et al., 1989). The smaller the size of the charcoal, the greater the surface of contact with the metaplast and, therefore, the greater the possibility of interaction between the matrix and the inert components. In addition, as the devolatilization intervals of

charcoal and coal overlap to some extent (Diez et al., 2012a; Alonso et al., 2001), the charcoal will emit oxygen-rich volatiles that can participate in the blockage of fluidity by establishing cross-linked O-C bonds. In summary, charcoal, being a high surface-area carbon solid, is able to adsorb a large variety of tarry substances which may promote interactions with the matrix. This gives rise to changes in the nature of the char-tar and coal-tar interactions and in the devolatilization rate, which will, in turn, affect the thermal behaviour patterns of the entire plastic stage of the coal. Both the Fmax and the plastic interval are affected by the addition of charcoal due to the increase in the softening temperature of the blend, which is sharper in the case of the finest fraction. The resolidification temperature, on the other hand, tends to decrease with the addition of charcoal, causing a further narrowing of the plastic interval, this effect also being greater in the case of the smallest size fraction.

3.4 Influence of coal inerts on the suppression of thermoplasticity with charcoal addition

Taking into account that coal thermoplasticity is the result of a combination of coalification (rank) and the genetic components (macerals) of coal, both factors should be considered to understand coal-char interactions during the transient plasticity phenomenon. It is well known that coal fluidity is not only controlled by the relative proportions of components that favor plasticity through physical and chemical processes (vitrinite and liptinite) and of inert components, which are physically passive (inertinite and mineral matter), but also by the rank-dependent thermoplastic properties of the vitrinite itself.

The fluid/plastic system could be considered as a three-phase system where gases, liquids, and solid particles coexist. Hence, the addition of solid inerts will modify fluidity through: i) varying the amount and chemical type of plastic components; ii) affecting the temperature-dependent

fluidity development; iii) the contribution of solid particles dispersed in the fluid matrix; and iv) the formation of trapped gases in the fluid phase. Considering that most of the unfused inertinite from coal probably remains in a solid state during the development of fluidity, the inertinite content of the base coal is a critical factor to be considered when incorporating additional inerts to the blend. An examination of the maceral composition of the coals studied reveals that coal MF, whose Fmax is the least affected by the addition of charcoal, has the lowest inertinite content (14.8 vol% *vs.* 17.6 and 22.2 vol% for coals HF and LF, respectively). Consequently coal MF is able to more easily assimilate a larger amount of suspended solids in the fluid matrix. Fig. 5 shows the variation in Fmax as a function of the total organic inerts in the parent blend. As the blends are prepared by weight but the maceral composition is quantified by volume, a weight-to-volume transformation for the charcoal was carried out using its density values (Table 3) in order to calculate the amounts of organic inerts by volume in the blends. All the values were adjusted to potential curves and both the effect of charcoal size and the amounts of organic inerts are important.

In the case of the curves of the coals with a moderate-to-low fluidity (MF and LF), the total amounts of organic inerts appear to explain the differences observed between them since the curves tend to converge at certain organic inert values. However, a rather different shape is observed for HF indicating that neither the properties of the vitrinite nor the amount of inerts by themselves can explain the behavior of the studied coals. One way to combine both variables is through the "Compositional Balance Index-CBI" as defined by Schapiro et al. (1961). This index is a quotient between the actual inerts in the coal and those calculated as optimum from a few experimental curves. The index is based on the principle that different vitrinites, with different fluidity properties, have different optimum reactive/inert ratios, making it possible to determine

whether a coal is short of inerts for reaching an optimum strength. The curve has a minimum reactive/inert ratio of 2.5 for a vitrinite reflectance of 0.9% and the ratio increases for lower and higher rank coals, reaching values of over 10 for coals with a vitrinite reflectance greater than 1.4%. Although the focus is on strength rather than on thermoplasticity, the CBI allows a comparison to be made between the capacity of vitrinite of different ranks to accept inerts. The CBI values of each coal are shown in Table 4 and indicate that MF is clearly short of inerts, whereas LF is in excess of the optimum amount even when no charcoal has been added. When the drop in fluidity is plotted vs CBI (Fig. 6), the ranking of the coals is similar to that observed in the plots of Fig. 4. This shows that MF is able to accept a higher amount of charcoal than either the HF or LF coals for a similar drop in fluidity, suggesting that if a coal is short of inerts, as determined by the CBI, a larger amount of charcoal can be added to this coal with only a minimal loss of fluidity. In Fig. 7, the loss in Fmax is plotted vs CBI for the three coals and the lines connect the values corresponding to different charcoal additions. A similar shape is observed in the curves for equivalent amounts of inerts despite the differences in the sizes of the charcoals added. The differences are larger for 2 and 5 wt% additions but the curves become closer for 10 and 15 wt% additions. Moreover, the differences between the losses in Fmax become minimal as the added charcoal sizes become smaller.

It is difficult to establish whether the size of the inertinite in the parent coal also plays a role in the drop in Fmax because the amounts of inertodetrinite (<10 μm) are rather small in all three coals (3 to 5 vol%) and because only minor differences between the three coals are observed. It is nevertheless worth noting that most of the inertinite in the coals will be in the size range of the

medium and coarse charcoals added to the blends and that the MF coal has the highest proportion of inertodetrinite.

3.5 Distinguishing charcoal and inertinite in the semicoke

Inertinite in coal is formed by more or less rapid processes of lignocellulosic tissue devolatilization and oxidation, on top of which coalification is superimposed due to heating and to lithostatic pressure. Charcoal can be considered as the fast partial devolatilization product of similar tissues which occurred in an oxygen-deficient atmosphere where the effect of coalification is lacking. The cell-lumens in the charcoal would then remain mostly undeformed both in high reflecting and low reflecting material, whereas they would be much more deformed in semifusinite, and less so in fusinite. Fusinite typically has a high polishing relief, which can also be expected in, at least, the highest reflecting charcoals. Inertinite, especially if it is of moderate size, could easily be integrated into the semicoke matrix, whereas the integration of charcoal would be very much dependent on blend homogenization before coking and the ability of the molten vitrinite to penetrate the structure of the charcoal. Some examples of inertinite and charcoal in the semicokes are shown in Fig. 8. The most relevant characteristic that distinguishes charcoal from isotropic inertinite is the higher polishing relief of the charcoal and the fact that the cell-lumens are often open and sometimes have not been infiltrated by the matrix. In addition, charcoal particles remained isotropic whereas inertinite may develop anisotropy during the semicoke formation, frequently with wavy-like extinction, although formation of anisotropic domains in the lowest reflecting inertinites has also been observed. The presence of certain anisotropy in organic inclusions can be considered a distinguishing feature for inertinite and these particles are typically well-integrated in the coke matrix and show low-to-moderate relief.

In the case of isotropic unfused components, and because it is difficult to unequivocally assign them to either charcoal or inertinite, the criterion of sharp edges was used as the main distinguishing feature in this study. Thus, smooth-edged particles of less than 20 μm probably derive from inertodetrinite whereas the sharp-edged particles are attributed to the finest charcoal. In addition, most of the smooth-edged inerts of more than 20 μm are derived from macrinite and semifusinite, while the sharp-edged particles in the size range of 80-212 μm are probably derived from charcoal. Fusinite also could yield particles with sharp or smooth edges depending on the accompanying components.

The different categories in which organic inerts have been split trying to assign the organic inerts present in the semicoke to the charcoal or the coal are shown in Tables 5, 6, and 7. The amount of inerts in the semicoke has also been estimated from the original amount in the parent coals. The steps involved in the estimation were as follows: i) calculation of the semicoke yields of charcoal and each maceral group (Borrego et al., 2000) considering that they retain 10% of the volatiles, and ii) normalization of the matrix and organic inert yields to a mineral matter free basis. The estimation of organic inert yields in the semicoke is plotted in Fig. 9 versus the actual amount determined by point counting. The plot shows that the calculated organic inerts are generally close to those quantified and that for small amounts of added charcoal the amounts quantified by point counting are generally lower than those predicted, whereas in the case of large additions the amounts actually quantified are larger than those calculated. Even assuming that the calculated values are subject to a certain degree of error due to the weight-to-volume transformations and to the fact that the coke yields of the maceral groups are derived from mathematical expressions, all the calculations will be subject to a similar degree of error and, therefore, the observed trends can be considered as consistent. These results suggest that

inertinite is more reactive when a limited amount of charcoal is added. In addition, the positive deviation of the organic inerts quantified by point-counting at high charcoal additions might indicate that in these conditions not only was any inertinite and charcoal identifiable as an inclusion, but also that minor vitrinite-derived semicoke matrix could have remained isotropic, being difficult to distinguish from organic inclusions.

3.6 Influence of charcoal on semicoke optical texture

To assess the effect of controlled-size charcoal addition to coal on the development of optical texture, the semicokes recovered from each Gieseler plastometer run were studied by optical microscopy. Several reasons justified the selection of the Gieseler semicokes: i) The coal composition is a key factor in the development of optical texture and porous structure of coal-based carbons and therefore the optical textures of semicoke and coke are closely related to the nature of the parent coal; ii) Most of the characteristics of high-temperature coke are established in the temperature range 350-500 ºC, and after the resolidification process, the organization of carbon arrangements in the semicoke is preserved under the usual conditions of coke oven operation (Loison et al. 1989); iii) Gieseler plastometry is a useful technique and widely used in research and industry when deciding which coal or additive to use in a blend for coke production and to predict coke quality; iv) Semicokes produced in dynamic and isothermal conditions in a Gieseler plastometer or in laboratory-scale ovens have provided valuable information on the development of optical texture as a function of coal properties (Hower and Lloyd, 1999) as well as on the mechanisms involved in the development of coal rheological properties with carbon-bearing additives (Grint et al., 1985; van Krevelen, 1993; Clemens and Matheson, 1995; Menendez et al. 1996; 1997; Sakurovs, 2000).

Tables 5 to 7 show the results obtained from the textural analyses performed on each of the 36 coal-charcoal blends. The semicoke matrix from the highest rank coal (LF) has the largest optical texture made up mainly of medium size domains (Table 5), whereas that from the lowest rank coal (HF) is made up of a combination of mosaics and domains (Table 7). The MF coal, that has a vitrinite reflectance value intermediate between the other two coals, yields the smallest optical texture in the semicoke which is dominated by fine-to-medium-size mosaics (Table 6). Overall, the amounts of sharp-edged inerts in the different size intervals are in good agreement with the sizes of the charcoal added to the coal.

The addition of 2 wt% charcoal to the coal causes a decrease in the size of the anisotropic components of the matrix. In the case of the LF and MF coals, a 2 wt% addition of charcoal produces an appreciable decrease in the size of the optical textures. This decrease is less important when the largest charcoal is added (CH212) but there is a reduction in domains of approximately 50% with the addition of CH80 and CH20. This decrease mainly affects the domains of largest size. The HF coal seems to be the least affected by the addition of small amounts of charcoal, which mainly involves the medium-size domain texture, while the amounts of fine domain texture remain more or less the same. Generally speaking, regardless of the optical texture of the charcoal-free semicoke, the addition of carbonized biomass causes a reduction in the optical size of the matrix, the extent of which depends on the amount of charcoal added. Both the amount and the size of the charcoal appear to play a relevant role and the addition of small particles of biomass causes a greater reduction in the size of the optical texture than the addition of large biomass particles. The reduction in texture size with the addition of charcoal is observed in all three semicokes but the semicoke with the smallest optical texture

(MF) is the least affected by this reduction. The reduction observed in the size of the texture may have significant implications for the reactivity of the coke and this effect may be accompanied by other possible effects resulting from the catalytic influence of mineral matter (MacPhee et al., 2009; Ng et al., 2011; Diez and Borrego, 2013), which are important in the present case due to the low mineral matter content of the charcoal used.

4. Conclusions

A systematic study of the addition of charcoal with a well-controlled size to good coking coals has revealed significant differences in the fluid properties of the coal-charcoal blends and the optical texture of the corresponding semicokes. The reduction in the fluidity of the coal when charcoal was added was not only dependent on the rank of the coal and the fluidity properties of the vitrinite, but also on the amount of inertinite and the optimum ratio of reactive-to-inert components within the coal. The coals with a higher reactive-to-inert ratio were able to incorporate a higher amount of charcoal as the effect on their thermoplastic properties was less detrimental.

The reduction in fluidity with the addition of charcoal was found to be related to the particle size of the charcoal. It was observed that the smaller the charcoal particles, the greater the suppression of fluidity. Additions of charcoal in the range of the particle sizes of this study caused a reduction in the optical texture of the semicokes that would enhance any increase in reactivity resulting from the addition of biomass. The addition of small charcoal particles of a similar size to inertodetrinite caused a greater reduction in the size of the optical textural components than the incorporation of larger charcoal particles.

Acknowledgements

The research leading to these results has received funding from the Research Programme of the Research Fund for Coal and Steel (Grant Agreement number RFC-PR- 09024). Co-financing from PCTI grant COF11-39 and funds from MICINN (PIB2010BZ-00418 project) are also acknowledged. J.C. Hower and two anonymous referees are thanked for revision and improvement of the manuscript.

Alonso, M.J.G., Alvarez, D., Borrego, A.G., Menendez, R., Marbán, G., 2001. Systematics effects of coal rank and type on the kinetics of coal pyrolysis. Energy Fuels 15, 413-428.

Ammossov, I.I., Eremin, I.V., Sukhenko, S.F., Oshurkova, L.S., 1957. Calculation of coking changes on basis of petrographic characteristics of coals. Coke Chemistry USSR 2, 9–12.

ASTM D2639/D2639M-13. Standard Test Method for Plastic Properties of Coal by the Constant-Torque Gieseler Plastometer, ASTM International, West Conshohocken, PA, 2013, www.astm.org

ASTM D5061-07. ASTM D5061-07, Standard Test Method for Microscopical Determination of the Textural Components of Metallurgical Coke, ASTM International, West Conshohocken, PA, 2007, www.astm.org

Barriocanal, C., Alvarez, R., Canga, C.S., Diez, M.A.,1998. On the possibility of using coking plant waste materials as additives for coke production. Energy Fuels 12, 981-989.

Borrego, A.G., Marbán, G., Alonso, M.J.G., Alvarez, D., Menendez, R., 2000. Maceral effects in the determination of proximate volatiles in coal. Energy Fuels 14, 117-126.

Butterfield, I.M., Thomas, K.M., 1995. Some aspects of changes in the macromolecular structure of coals in relation to thermoplastic properties. Fuel 74, 1780-1785.

Castro Díaz, M., Zhao, H., Kokonya, S., Dufour, A., Snape, C.E., 2012. The effect of biomass on fluidity development in coking blends using High-Temperature SAOS Rheometry. Energy Fuels 26, 1767-1775.

Choudhury, N., Mohanty, D., Boral, P., Kumar, S., Hazra, S.K., 2008. Microscopic evaluation of coal and coke for metallurgical usage. Current Science 94, 74-81.

Clemens, A.H., Matheson, T.W., 1995. The effect of selected additives and treatments on Gieseler fluidity in coals. Fuel 74, 57–62.

Diessel, C.F.K., 1983. Carbonization reactions of inertinite macerals in Australian coals. Fuel 62, 883–892.

Diessel, C.F.K., 1992. Coal and Coal-bering depositional systems. Springer-Verlag, Berlin. 721 pp.

Diessel, C.F.K., Wolff-Fischer, E., 1986. Vergleichsuntersuchungen an Kohlen und Koksen zur Frage der Inertinitreaktivität. Glückauf Forsch. 47, 203-211.

Diessel, C.F.K., Wolff-Fischer, E., 1987. Coal and coke petrographic investigations into the fusibility of Carbonaceous and Permian coking Coals. Int. J. Coal Geol. 9, 87-108.

Diez, M.A., 2014. Metallurgical coke. In Encyclopedia of Iron, Steel and their Alloys, Colás R. and Totten, G.E. (eds), Taylor and Francis Group, New York, USA, in press. (DOI: 10.1081/E-EISA-120050908).

Diez, M.A, Alvarez, R., 2013. Advances in the recycling of plastic wastes for metallurgical coke production. J. Mater. Cycles Waste 15, 247 -255.

Diez, M.A., Borrego, A.G., 2013. Evaluation of CO_2-reactivity patterns in cokes from coal and woody biomass blends. Fuel 113, 59-68.

Diez, M.A., Barriocanal, C., Alvarez, R., 2005. Plastic wastes as modifiers of the thermoplasticity of coal. Energy Fuels 19, 2304-2316.

Diez, M.A., Alvarez, R., Melendi, S., Barriocanal, C., 2009. Feedstock recycling of plastic wastes/oil mixtures in cokemaking. Fuel 88, 1937-1944.

Diez, M.A., Alvarez, R., Fernandez, M., 2012a. Biomass derived products as modifiers of the rheological properties of coking coals. Fuel 96, 306-313.

Diez, M.A., Smatanova, N., Rodríguez, E., Borrego, A.G., 2012b. Influence of woody biomass on coal thermoplasticity. Proc. 64rd Annual Meeting of the ICCP, 2012, Beijing, China, (CD-version).

Fernandez, A.M., Barriocanal, C., Diez, M.A, Alvarez, R., 2009. Influence of additives of various origins on thermoplastic properties of coal. Fuel 88, 2365–2372.

Fortin, F., Rouzaud, J.N., 1993. The role of the molecular component in coke microtexture formation. Fuel 72, 245-250.

Fortin, F., Rouzaud, J.N., 1994. Different mechanisms of coke microtexture formation during coking coal carbonization. Fuel 73, 795-809.

Fukuyama, T., Funabiki, Y., Itagaki, S., 1981. Estimation of coke properties using petrographic analysis of semi-coke. J. Fuel Soc. Japan 60, 174-182.

Gan, H., Nandi, S.P., Walker, P.L. Jr. 1972. Nature of the porosity in American coals. Fuel 51, 272-277

Gransden, J.F., Jorgensen, J.G., Manery, N., Price, J.T., Ramey, N.J., 1991. Application of microscopy to coke making. Int. J. Coal Geol. 19, 77-107.

Gray, R.J., Devanney, K.F., 1986. Coke carbon forms: Microscopic classification and industrial applications Int. J. Coal Geol. 6, 277-297

Grint, A., Mehani, S., Trewhella, M., Crook, M.J., 1985. Role and composition of the mobile phase in coal. Fuel 64, 1355-1361.

Guerrero, A., Diez, M.A.; Borrego, A.G. 2013. Effect of volatile matter release on optical properties of macerals from different rank coals. Fuel 114, 21-30.

Hanrot, F., Sert, D., Delinchant, J., Pietruck, R., Bürgler, T., Babich, A., Fernandez, M., Alvarez, R., Diez, M.A., 2009. CO_2 mitigation for steelmaking using charcoal and plastics wastes as

reducing agents and secondary raw materials. Proc. 1st Spanish National Conf. on Advances in Materials Recycling and Eco–Energy. Recimat 09, paper S05-4. Available at: http://hdl.handle.net/10261/18433.

Hower, J.C., Lloyd, W.G., 1999. Petrographic observations of Gieseler semi-cokes from high volatile bituminous coals. Fuel 78, 445-451.

International Committee for Coal and Organic Petrology (ICCP), 1998. The new vitrinite classification (ICCP System 1994). Fuel 77, 349–538.

International Committee for Coal and Organic Petrology (ICCP), 2001. The new inertinite classification (ICCP System 1994). Fuel 80, 459–71.

ISO 17246:2010. Coal-Proximate analysis. International Organization for Standardization, Geneva, Switzerland.

ISO 29541:2010. Solid mineral fuels -Determination of total carbon, hydrogen and nitrogen content -Instrumental method. International Organization for Standardization, Geneva, Switzerland.

ISO 19579:2006. Solid mineral fuels - Determination of sulfur by IR spectrometry. International Organization for Standardization, Geneva, Switzerland.

ISO 7404-5:2009 . Methods for the petrographic analysis of coals -Part 5: Method of determining microscopically the reflectance of vitrinite. International Organization for Standardization, Geneva, Switzerland.

ISO 7404-3:2009. Methods for the petrographic analysis of coals - Part 3: Method of determining maceral group composition. International Organization for Standardization, Geneva, Switzerland.

Komorek, J., Morga, R., 2007. Evolution of optical properties of vitrinite, sporinite and semifusinite in response to heating under inert conditions. Int. J. Coal Geol. 71, 389-404.

Krevelen D.W. van 1993. Coal: Typology–Physics–Chemistry–Constitution (3rd edn.). Elsevier, Amsterdam, 979 pp.

Loison, R., Foch, P., Boyer, A., 1989. Coke quality and production. Butterworth, London, 353 pp.

Mackowsky, M-Th., 1977. Prediction methods in coal and coke microscopy. J. Microsc-Oxford 109, 119–136.

MacPhee, J.A., Gransden, J.F., Giroux, L., Price, J.T., 2009. Possible CO_2 mitigation via addition charcoal to coking coal blends. Fuel Proc. Technol. 90, 16-20.

Marsh, H. 1992. The cokemaking process. AIME Ironmaking Proc. 51, Toronto, 569–580.

Mendez, L.B., Borrego, A.G., Martinez-Tarazona, M.R., Menendez, R., 2003. Influence of petrographic and mineral matter composition of coal particles on their combustion reactivity. Fuel 82, 1875–1882.

Menendez, J.A, Pis J.J., Alvarez, R., Barriocanal, C., Fuente, E., Diez, M.A., 1996. Characterization of petroleum coke as an additive in metallurgical cokemaking. Modification of thermoplastic properties of coal. Energy Fuels 20, 1262-1268.

Menendez, J.A., Pis, J.J., Alvarez, R., Barriocanal, C., Canga, C.S., Diez, M.A., 1997. Characterization of petroleum coke as an additive in metallurgical cokemaking. Influence on metallurgical coke quality. Energy Fuels 11, 379-384.

Miyazu, T., 1974. The evaluation and design of blends using many kinds of coals for cokemaking. Int. Iron Steel Cong., Dusseldorf, Pap. 1.2.2.1.

Montiano, M.G., Barriocanal, C., Alvarez, R., 2013. Effect of the addition of waste sawdust on thermoplastic properties of a coal. Fuel 106, 537-543.

Murchison, D.G., 1991. Petrographic aspect of coal structure: reactivity of maceral in laboratory and natural environment. Fuel 70, 296– 315.

Ng, K.W., MacPhee, J.A., Giroux, L., Todoschuk, T., 2011. Reactivity of bio-coke with CO_2, Fuel Proc. Technol. 92, 801-804.

Ng, K.W., Giroux, L., MacPhee, J.A., Todoschuk, T., 2012. Incorporation of charcoal in coking coal blend-A study of the effects on carbonization conditions and coke quality. 2012 AISTech Conf. Proc., 13pp.

Patrick, J.W., 1975. Recent developments in understanding the fundamental aspects of the coking process. In: The Coke Oven Managers' Association (COMA) Year-Book, Mexborough, UK, 201-263.

Patrick, J.W., Reynolds, M.J., Shaw, F.H., 1973. Development of optical anisotropy in vitrains during carbonization. Fuel 52, 198-204.

Patrick, J.W., Reynolds, M.J., Shaw, F.H., 1979. Optical anisotropy of carbonized coking-coal and caking-coal vitrains. Fuel 58, 501-509.

Pearson, D.E., Price, J.T., 1985. Reactivity of inertinite (coal typing) of western Canadian coking coal. Int. Conf. Coal Sci. Sydney, 907-908.

Pohlmann, J.G., Osório, E., Vilela, A.C.F., Borrego, A.G. 2010. Reactivity to CO_2 of chars prepared in O_2/N_2 and O_2/CO_2 mixtures for pulverized coal injection (PCI) in blast furnace in relation to char petrographic characteristics. Int. J. Coal Geol. 84, 293-300.

Pusz, S., Kwiecinska, B., Koszorek, A., Krzesinska, M., Pilawa, B. 2009 Relationships between the optical reflectance of coal blends and the microscopic characteristics of their cokes, Int. J. Coal Geol. 77, 356-362.

Sakurovs, R., 2000. Some factors controlling the thermoplastic behaviour of coals, Fuel 79, 379-389.

Schapiro, N., Gray, R.J., Eusner, G.R., 1961. Recent developments in coal petrography. AIME Blast Furnace Coke Oven and Raw Material. Proc. 20, 89-112.

Scott, A.C., Glasspool, I.J., 2007. Observations and experiments on the origin and formation of inertinite group macerals. Int. J. Coal Geol. 70, 53-66.

Taylor, G.H., Mackowsky, M-Th., Alpern, B., 1967. The behaviour of inertinite during carbonisation. Fuel 46, 431–440.

Taylor, G.H., Liu, S.Y., Diessel, C.F.K., 1989. The cold-climate origin of inertinite-rich Gondwana coals. Int. J. Coal Geol. 11, 1-22.

Ueda, S., Watanabe, K., Yanagiya, K., Inoue, R., Ariyama, T., 2009. Optimization of biomass utilization for reducing CO_2 in ironmaking process. J. Iron Steel Res. Int. 16, 593–599.

Valia, H.S., Hooper, W., 1994. Use of reverts and non-coking coals in metallurgical coke making. ISS Ironmaking Conf. Proc. 53, 89–105.

Figure Captions

Fig. 1. Schematic diagram of charcoal fraction separation method by the wet sieving process

Fig. 2. SEM and microphotographs images of the charcoals of different size: a.d) CH20; b.e) CH80; c.f) CH212.

Fig. 3. Variation in the fluidity of the blends with the amount and size of the charcoal added

Fig. 4. Percentage loss of Fmax for the LF, MF and HF coals as a function of charcoal amount and size

Fig. 5. Variation of Gieseler Fmax with the total amount of organic inerts (charcoal + Inertinite group macerals)

Fig. 6. Loss in Gieseler fluidity in relation to the Compositional Balance Index (CBI)

Fig. 7. Shape of the loss in fluidity curves corresponding to different charcoal additions as a function of the Compositional Balance Index (CBI) for the three size fractions

Fig. 8. Photomicrographs of the semicokes obtained in a Gieseler plastometer showing the inertinite inclusions (In) and charcoal inclusions (Ch)

Fig. 9. Organic inerts quantified in the semicoke vs. those calculated using the maceral composition of the coals and the normalized semicoke yields of Table 4

Table 1. Main characteristics of the coals and charcoal studied.

Coal	LF	MF	HF	CH
Volatile matter (wt% db)	19.3	23.8	24.7	22.37
Volatile matter (wt% daf)	21.2	26.3	27.2	23.4
Ash (wt% db)	8.9	9.5	9.1	4.3
Mineral matter calculated using Parr formula (wt %)	9.9	10.8	10.2	4.6
ρHe Coal (g/cm^3)	1.38	1.37	1.36	1.48
ρHe Organic matter (g/cm^3)	1.24	1.20	1.20	1.43
Elemental composition (wt%)				
St db	0.58	0.95	0.62	0.03
C daf	91.92	89.13	87.65	82.48
H daf	4.99	5.12	5.23	2.82
N daf	1.93	1.54	2.37	0.67
$(O+S_{org})_{dif}$ daf	1.15	4.21	4.76	14.03
Gieseler fluidity Parameters				
Fmax (ddpm)	373	541	1891	
Ts (ºC)	419	406	397	
Tf (ºC)	461	457	457	
Tr (ºC)	497	493	493	
Plastic range (ºC)	78	87	96	

wt=weight; db=dry basis; daf=dry-ash-free basis; ρHe=Helium density; Fmax=Maximum fluidity;Ts=softening temperature; Tf=temperature of maximum fluidity; Tr=resolidification temperature.

Table 2. Petrographic (maceral and reflectance) analyses of the different components of the coals (vol=volume; Rr=random reflectance).

Coal	LFC		MFC		HFC	
	vol (%)	Rr (%)	vol (%)	Rr (%)	vol (%)	Rr (%)
Vitrinite	76.8	1.25	82.8	1.22	81.1	1.17
Telovitrinite	70.4	1.25	73.8	1.22	78.2	1.18
Detrovitrinite	6.4	1.25	9.0	1.19	2.9	1.16
Inertinite	22.2	2.03	14.8	1.93	17.6	1.90
Fusinite	4.4	2.66	1.6	2.70	3.4	2.30
Semifusinite	12.4	1.79	7.0	1.84	9.4	1.69
Macrinite	1.4	2.16	1.0	2.18	1.6	2.34
Inertodetrinite	4.0	2.07	5.2	1.82	3.2	1.87
Liptinite	0.8	0.89	1.8	0.92	-	-
Coke	0.2	9.33	0.6	3.92	1.3	4.65

Table 3. Some chemical and physical parameters of the charcoal fractions

Parameter	**CH212**	**CH80**	**CH20**
Ash (wt% db)	3.05	3.16	4.81
ρHe charcoal (g cm^{-3})	1.47	1.48	1.50
ρHe Organic matter (g cm^{-3})	1.43	1.43	1.43
Coulter size-distribution			
Frequency <2 μm (%)	-	-	3.2
Frequency 2-10 μm (%)	-	1.0	47.7
Frequency 2-25 μm (%)	-	9.5	44.3
Frequency 25-50 μm (%)	-	39.5	4.8
Frequency 50-100 μm (%)	10.7	46.6	-
Frequency 100-200 μm (%)	67.7	3.4	-
Frequency >200 μm (%)	21.6	-	-
Mean size (μm)	189	60	12
Mode size (μm)	147	66	10

wt=weight; db=dry basis; daf=dry-ash-free basis; ρHe=Helium density

Table 4. Volatile matter (VM) content (daf %) of the maceral groups for each coal calculated from Borrego et al. (2000) and normalized semicoke yields (NSCy) of the different macerals

	LF	MF	HF
VMvitrinite	28.4	29.1	30.2
VMinertinite	19.4	19.6	19.9
VMliptinite	30.1	31.5	33.5
NSCkyvitrinite	75.1	81.2	79.9
NSCkyinertinite	24.0	16.8	20.1
NSCkyliptinite	0.9	2.1	0.0

Table 5. Optical texture (vol %) analyses of semicokes from LF coal. Values in bold refer to the percentage of the component in the sample and the other values to the percentage relative to the matrix or inert organic inclusions, depending on their class.

Blend	LF	LF212	LF212	LF212	LF212	LF80	LF80	LF80	LF80	LF20	LF20	LF20	LF20
Charcoal (%)	0	2	5	10	15	2	5	10	15	2	5	10	15
MATRIX	**71.6**	**72.8**	**71.1**	**65.2**	**59.4**	**70.2**	**66.2**	**64.4**	**57.0**	**73.2**	**65.2**	**53.8**	**54.1**
Isotropic (I)	2.3	5.7	3.5	5.0	5.0	5.4	5.4	10.2	10.7	6.3	2.4	11.1	17.1
Incipient anisotropic (Ia)	1.1	2.5	0.3	0.0	2.4	4.3	4.8	9.0	9.9	4.6	1.8	10.4	16.3
Mosaic	3.1	3.8	1.9	8.3	17.5	41.3	20.2	63.7	42.0	39.6	16.6	39.3	51.5
Fine (fM)	*0.0*	*0.0*	*0.0*	*1.2*	*2.4*	*15.1*	*5.1*	*26.7*	*14.5*	*9.8*	*3.1*	*15.2*	*19.7*
Medium (mM)	*2.0*	*1.9*	*0.6*	*1.8*	*7.4*	*21.4*	*4.5*	*34.5*	*15.3*	*23.2*	*6.4*	*14.8*	*18.6*
Coarse (cM)	*1.1*	*1.9*	*1.3*	*5.2*	*7.7*	*4.8*	*10.6*	*2.5*	*12.2*	*6.6*	*7.1*	*9.3*	*13.3*
Domain	93.1	89	95.3	86.8	74.1	51.6	74.0	25.5	46.6	53.8	75.8	46.7	27.7
Fine (fD)	*7.7*	*8.2*	*12.3*	*20.6*	*26.6*	*29.1*	*35.6*	*17.4*	*26.7*	*25.1*	*27.0*	*18.9*	*12.5*
Medium (mD)	*75.7*	*73.6*	*74.8*	*57.1*	*34.0*	*15.7*	*32.6*	*7.5*	*17.2*	*23.0*	*38.7*	*24.8*	*11.7*
Coarse (cD)	*9.7*	*7.1*	*8.2*	*9.2*	*13.5*	*6.8*	*5.7*	*0.6*	*2.7*	*5.7*	*10.1*	*3.0*	*3.4*
Fibers	2.0	3.0	0.9	2.5	4.7	2.3	0.6	1.2	1.1	1.1	5.5	3.3	4.2
Fine (fF)	*2.0*	*3.0*	*0.6*	*2.5*	*4.7*	*1.1*	*0.3*	*0.6*	*1.1*	*0.8*	*4.6*	*2.6*	*3.8*
Medium (mF)	*0.0*	*0.0*	*0.3*	*0.0*	*0.0*	*0.9*	*0.0*	*0.6*	*0.0*	*0.3*	*0.9*	*0.7*	*0.4*
Coarse (cF)	*0.0*	*0.0*	*0.0*	*0.0*	*0.0*	*0.3*	*0.3*	*0.0*	*0.0*	*0.0*	*0.0*	*0.0*	*0.0*
INCLUSIONS	**26.8**	**25.6**	**28.0**	**33.2**	**39.4**	**27.2**	**31.6**	**33.8**	**41.3**	**25.4**	**32.2**	**45.0**	**44.5**
Smooth-edged inerts (SMEI)	71.0	64.8	57.6	48.2	40.6	53.7	36.7	39.6	24.7	50.4	45.3	38.5	33.2
Inertodetrinite	18.3	14.8	9.6	8.4	11.2	14.7	15.2	9.5	8.4	14.2	13.7	12.8	7.8
Sharp edged inerts (SHEI)	10.7	19.5	30.4	40.4	44.7	30.9	47.5	49.7	64.7	33.9	39.8	48.7	59.0
212-80 µm	*6.1*	*10.9*	*20.8*	*33.1*	*35.5*	*7.4*	*10.8*	*5.3*	*7.9*	*7.1*	*5.0*	*4.4*	*1.8*
80-20 µm	*2.3*	*5.5*	*6.4*	*4.8*	*7.6*	*14.0*	*25.9*	*33.1*	*46.3*	*10.2*	*3.7*	*3.1*	*6.0*
<20 µm	*2.3*	*3.1*	*3.2*	*2.4*	*1.5*	*9.6*	*10.8*	*11.2*	*10.5*	*16.5*	*31.1*	*41.2*	*51.2*
Undifferentiated Isotropic Inclusions	**0.0**	**0.8**	**2.4**	**3.0**	**3.6**	**0.7**	**0.6**	**1.2**	**2.1**	**1.6**	**1.2**	**0.0**	**0.0**
Mineral Matter	**1.6**	**1.6**	**0.9**	**1.6**	**1.2**	**2.6**	**2.2**	**1.8**	**1.7**	**1.4**	**2.6**	**1.2**	**1.4**

Table 6

Table 6. Optical texture (vol %) analyses of semicokes from MF coal. Values in bold refer to the percentage of the component in the sample and the other values to the percentage relative to the matrix or inert organic inclusions, depending on their class.

Blend	MF	MF212	MF212	MF212	MF212	MF80	MF80	MF80	MF80	MF20	MF20	MF20	MF20
Charcoal (%)	0	2	5	10	15	2	5	10	15	2	5	10	15
MATRIX	**84.8**	**82.6**	**79.8**	**72.8**	**66.2**	**80.6**	**78.2**	**71.0**	**65.8**	**81.6**	**72.5**	**70.6**	**71.3**
Isotropic (I)	7.1	6.3	10.6	7.1	7.9	4.7	7.2	5.3	6.7	4.9	15.1	2.8	11.2
Incipient anisotropic (Ia)	*4.7*	*5.8*	*8.0*	*2.7*	*6.6*	*3.7*	*5.6*	*3.1*	*4.9*	*3.4*	*12.8*	*2.8*	*6.1*
Mosaic	68.4	79.2	72.7	76.8	83.7	85.6	70.6	81.4	86.6	84.8	69.3	90.1	86.3
Fine (fM)	*39.4*	*46.2*	*46.6*	*50.0*	*71.6*	*53.8*	*52.4*	*52.4*	*72.6*	*56.4*	*54.7*	*64.6*	*68.4*
Medium (mM)	*21.2*	*28.6*	*19.8*	*25.7*	*12.1*	*31.5*	*15.3*	*27.3*	*13.4*	*27.2*	*12.3*	*23.2*	*15.4*
Coarse (cM)	*7.8*	*4.4*	*6.3*	*1.1*	*0.0*	*0.2*	*2.8*	*1.7*	*0.6*	*1.2*	*2.2*	*2.3*	*2.5*
Domain	25.5	14.3	18.0	18.0	8.2	9.4	22.8	14.1	7.6	11.0	16.8	7.1	5.0
Fine (fD)	*16.0*	*11.1*	*12.5*	*12.6*	*6.3*	*7.4*	*15.6*	*11.0*	*6.1*	*9.3*	*11.7*	*6.8*	*3.9*
Medium (mD)	*6.8*	*2.9*	*4.5*	*4.6*	*1.5*	*1.7*	*6.9*	*3.1*	*1.5*	*1.7*	*4.7*	*0.3*	*1.1*
Coarse (cD)	*2.6*	*0.2*	*1.0*	*0.8*	*0.3*	*0.2*	*0.3*	*0.0*	*0.0*	*0.0*	*0.3*	*0.0*	*0.0*
Fibers	0.2	0.5	0.0	0.3	0.9	0.7	0.3	0.3	0.0	0.0	0.0	0.0	0.0
Fine (fF)	*0.0*	*0.5*	*0.0*	*0.3*	*0.9*	*0.7*	*0.3*	*0.3*	*0.0*	*0.0*	*0.0*	*0.0*	*0.0*
Medium (mF)	*0.0*	*0.0*	*0.0*	*0.0*	*0.0*	*0.0*	*0.0*	*0.0*	*0.0*	*0.0*	*0.0*	*0.0*	*0.0*
Coarse (cF)	*0.2*	*0.0*	*0.0*	*0.0*	*0.0*	*0.0*	*0.0*	*0.0*	*0.0*	*0.0*	*0.0*	*0.0*	*0.0*
INCLUSIONS	**11.8**	**15.8**	**17.8**	**25.8**	**31.2**	**17.6**	**19.8**	**27.6**	**32.6**	**17.4**	**22.9**	**27.6**	**27.1**
Smooth edges Inerts (SMEI)	35.6	38.0	24.7	23.1	17.9	44.3	27.3	25.4	16.0	27.6	30.1	24.6	22.1
Inertodetrinite	18.6	11.4	16.9	7.7	6.4	13.6	11.1	6.5	5.5	13.8	14.2	6.5	4.4
Sharp edges Inerts (SHEI)	45.8	50.6	53.9	69.2	71.2	42.0	59.6	68.1	77.9	58.6	54.9	68.8	73.5
212-80 µm	*13.6*	*32.9*	*27.0*	*49.2*	*46.2*	*12.5*	*8.1*	*10.1*	*4.3*	*16.1*	*6.2*	*5.1*	*0.7*
80-20 µm	*18.6*	*10.1*	*13.5*	*16.2*	*19.2*	*20.5*	*37.4*	*49.3*	*51.5*	*3.4*	*2.7*	*5.1*	*3.7*
<20 µm	*13.6*	*7.6*	*13.5*	*3.8*	*5.8*	*9.1*	*14.1*	*8.7*	*22.1*	*39.1*	*46.0*	*58.7*	*69.1*
Undifferentiated Isotropic Inclusions	**0.0**	**0.0**	**4.5**	**0.0**	**4.5**	**0.0**	**2.0**	**0.0**	**0.6**	**0.0**	**0.9**	**0.0**	**0.0**
Mineral Matter	**3.4**	**1.6**	**2.4**	**1.4**	**2.6**	**1.8**	**2**	**1.4**	**1.6**	**1.0**	**4.7**	**1.8**	**1.6**

Table 7

Table 7. Optical texture (vol %) analyses of semicokes from HF coal. Values in bold refer to the percentage of the component in the sample and the other values to the percentage relative to the matrix or inert organic inclusions, depending on their class.

Blend	HF	HF212	HF212	HF212	HF212	HF80	HF80	HF80	HF80	HF20	HF20	HF20	HF20
Charcoal (%)	0	2	5	10	15	2	5	10	15	2	5	10	15
MATRIX	**80.0**	**81.8**	**77.0**	**74.8**	**64.8**	**79.8**	**72.5**	**70.8**	**64.6**	**80.4**	**67.8**	**71.6**	**64.0**
Isotropic (I)	10.3	0.5	11.4	3.8	2.8	5.3	9.1	2.3	0.6	1.4	16.5	3.6	4.1
Incipient anisotropic (Ia)	*6.8*	*0.5*	*10.8*	*1.6*	*1.5*	*2.3*	*8.0*	*1.1*	*0.6*	*1.0*	*15.3*	*1.4*	*4.1*
Mosaic	31.3	53.3	30.7	79.1	60.8	47.4	37.2	75.4	77.7	59.0	29.5	79.6	81.6
Fine (fM)	*13.5*	*20.3*	*12.2*	*45.5*	*26.2*	*13.8*	*18.7*	*27.1*	*31.3*	*26.9*	*15.9*	*43.9*	*51.6*
Medium (mM)	*12.0*	*32.0*	*10.2*	*31.0*	*31.5*	*28.6*	*14.3*	*45.8*	*43.7*	*29.4*	*10.3*	*34.1*	*29.1*
Coarse (cM)	*5.80*	*1.00*	*8.30*	*2.70*	*3.10*	*5.00*	*4.10*	*2.50*	*2.80*	*2.70*	*3.20*	*1.70*	*0.90*
Domain	59.5	45.5	56.5	17.4	36.1	47.4	54.3	22.9	21.7	39.6	54.6	17.9	14.1
Fine (fD)	*29.5*	*30.3*	*34.9*	*12.6*	*26.2*	*31.3*	*43.3*	*19.5*	*17.6*	*29.6*	*40.4*	*13.7*	*13.1*
Medium (mD)	*23.8*	*12.5*	*17.2*	*3.7*	*8.0*	*12.0*	*9.4*	*3.4*	*3.1*	*8.2*	*13.0*	*3.6*	*0.9*
Coarse (cD)	*6.3*	*2.7*	*4.4*	*1.1*	*1.9*	*4.0*	*1.7*	*0.0*	*0.9*	*1.7*	*1.2*	*0.6*	*0*
Fibers	0.8	0.7	1.7	0.8	0.9	1.5	0.0	0.0	0.0	0.2	0.0	0.0	0.3
Fine (fF)	*0.8*	*0.5*	*1.7*	*0.5*	*0.9*	*0.8*	*0.0*	*0.0*	*0.0*	*0.2*	*0.0*	*0.0*	*0.0*
Medium (mF)	*0.0*	*0.2*	*0.0*	*0.3*	*0.0*	*0.8*	*0.0*	*0.0*	*0.0*	*0.0*	*0.0*	*0.0*	*0.3*
Coarse (cF)	*0.0*	*0.0*	*0.0*	*0.0*	*0.0*	*0.0*	*0.0*	*0.0*	*0.0*	*0.0*	*0.0*	*0.0*	*0.0*
INCLUSIONS	**18.6**	**16.4**	**20.3**	**24.2**	**33.4**	**18.4**	**24.6**	**27.8**	**34.2**	**18.0**	**30.0**	**26.6**	**35.4**
Smooth edges Inerts (SMEI)	30.1	46.3	23.2	24.8	19.8	32.6	42.3	23.7	20.5	41.1	26.7	25.6	21.5
Inertodetrinite	12.9	9.8	10.5	5.8	7.8	10.9	5.7	8.6	7.0	14.4	9.3	6.8	8.5
Sharp edges Inerts (SHEI)	36.6	41.5	54.7	67.8	70.1	54.3	46.3	66.9	72.5	42.2	56.0	66.9	68.9
212-80 µm	*10.8*	*34.1*	*38.9*	*45.5*	*51.5*	*10.9*	*10.6*	*5.8*	*11.1*	*11.1*	*5.3*	*7.5*	*1.7*
80-20 µm	*12.9*	*3.7*	*13.7*	*15.7*	*14.4*	*34.8*	*22.8*	*45.3*	*50.3*	*7.8*	*8.0*	*4.5*	*4.0*
<20 µm	*12.9*	*3.7*	*2.1*	*6.6*	*4.2*	*8.7*	*13.0*	*15.8*	*11.1*	*23.3*	*42.7*	*54.9*	*63.3*
Undifferentiated Isotropic Inclusions	**20.4**	**2.4**	**11.6**	**1.7**	**2.4**	**2.2**	**5.7**	**0.7**	**0.0**	**2.2**	**8.0**	**0.8**	**1.1**
Mineral Matter	**1.4**	**1.8**	**2.8**	**1.0**	**1.8**	**1.8**	**3.0**	**1.4**	**1.2**	**1.6**	**2.2**	**1.8**	**0.6**

Figure 1

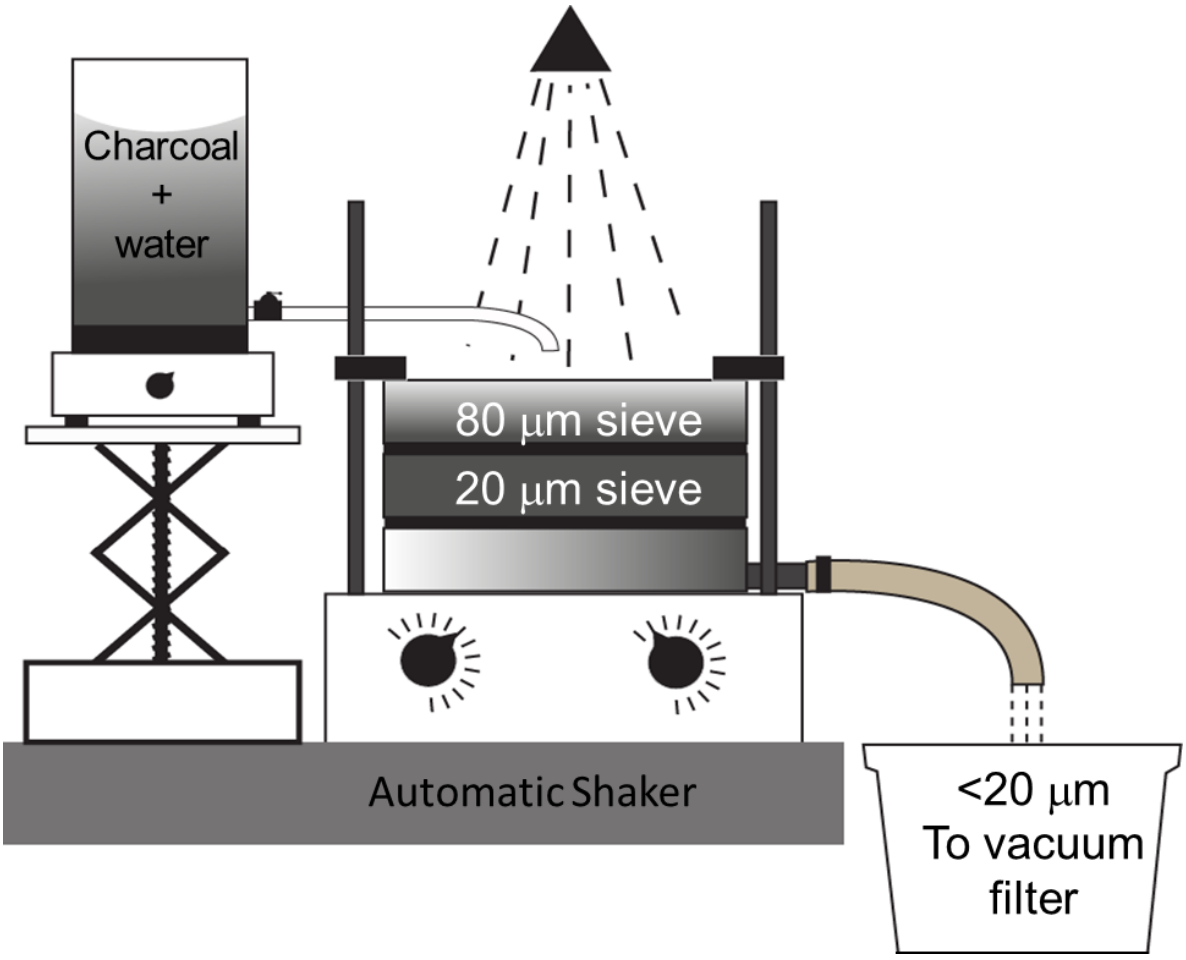

Fig.1

Figure 2

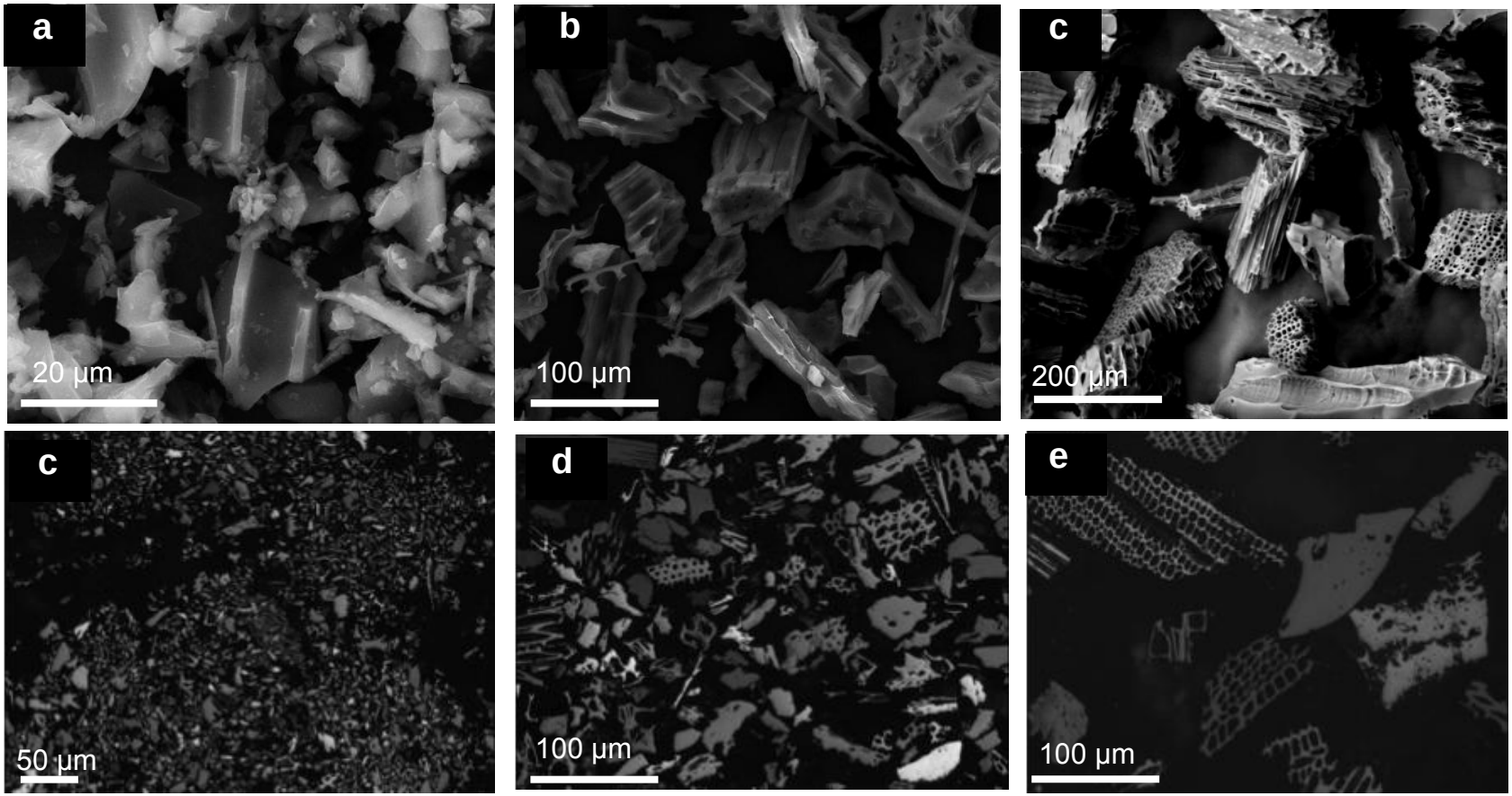

Fig.2

Figure 3

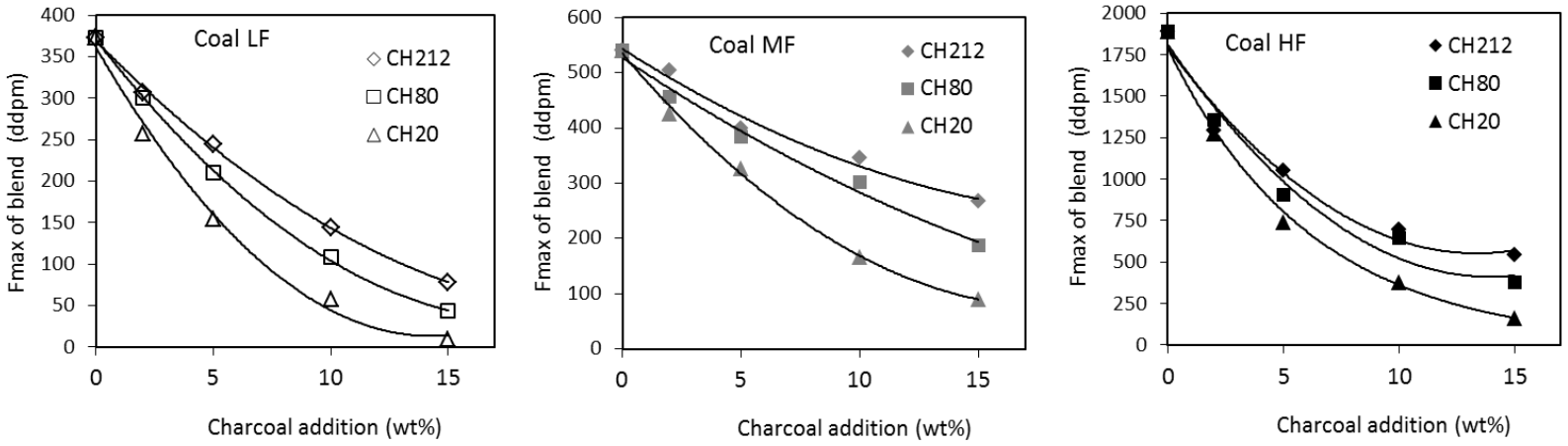

Fig.3

Figure 4

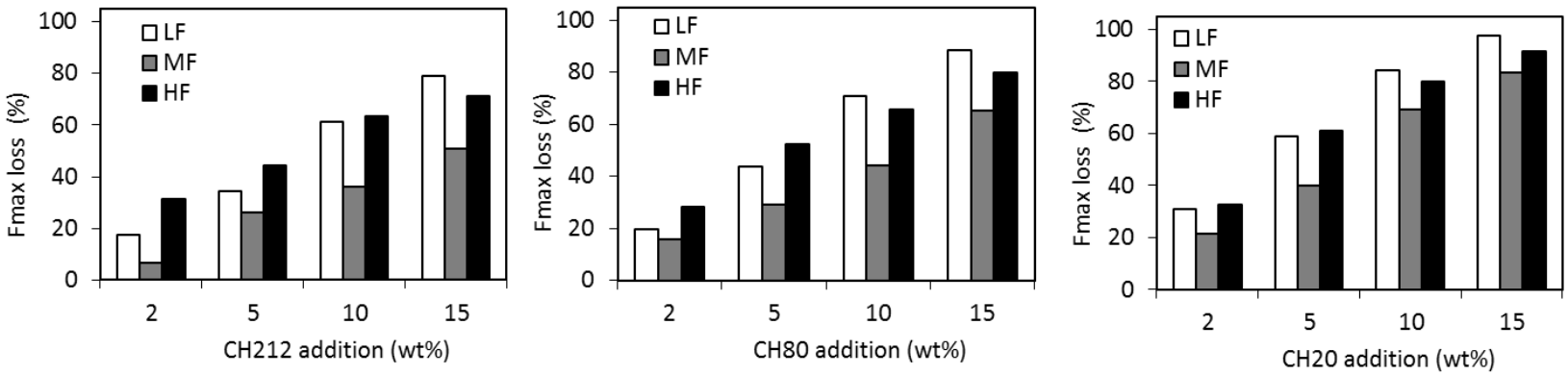

Fig.4

Figure 5

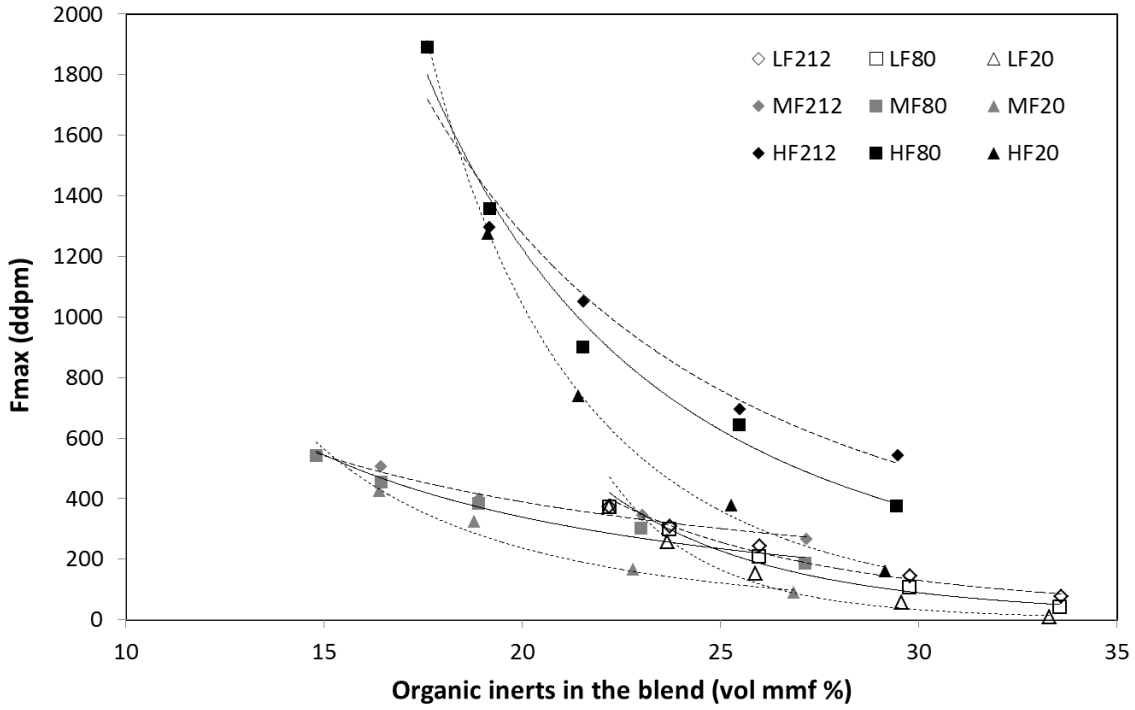

Fig.5

Figure 6

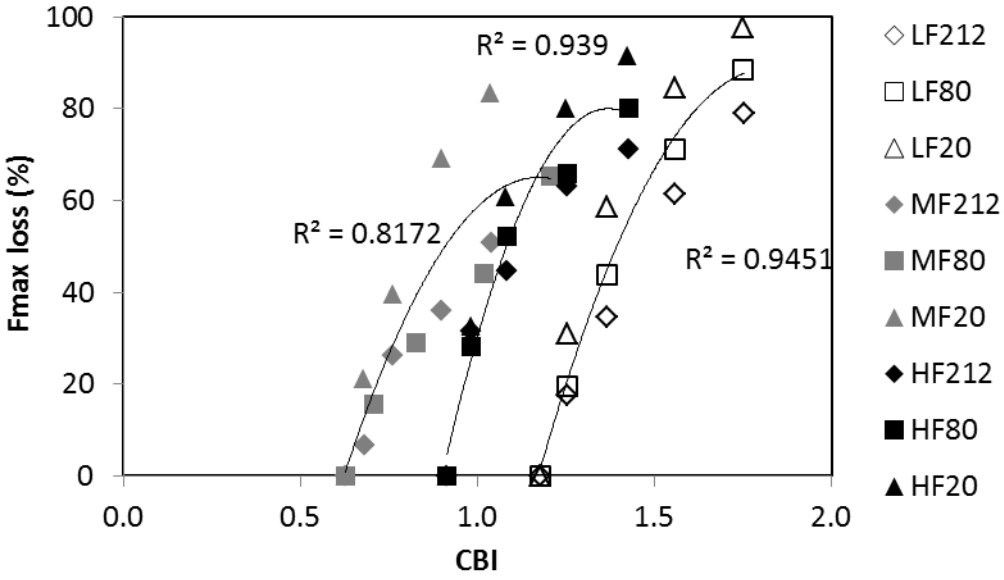

Fig.6

Figure 7

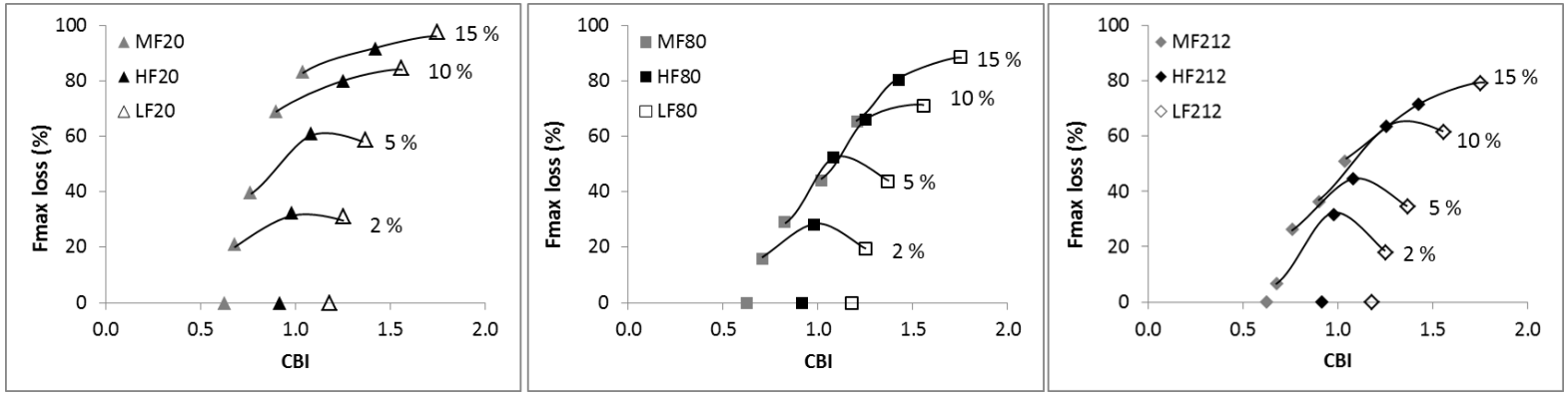

Fig.7

Figure 8

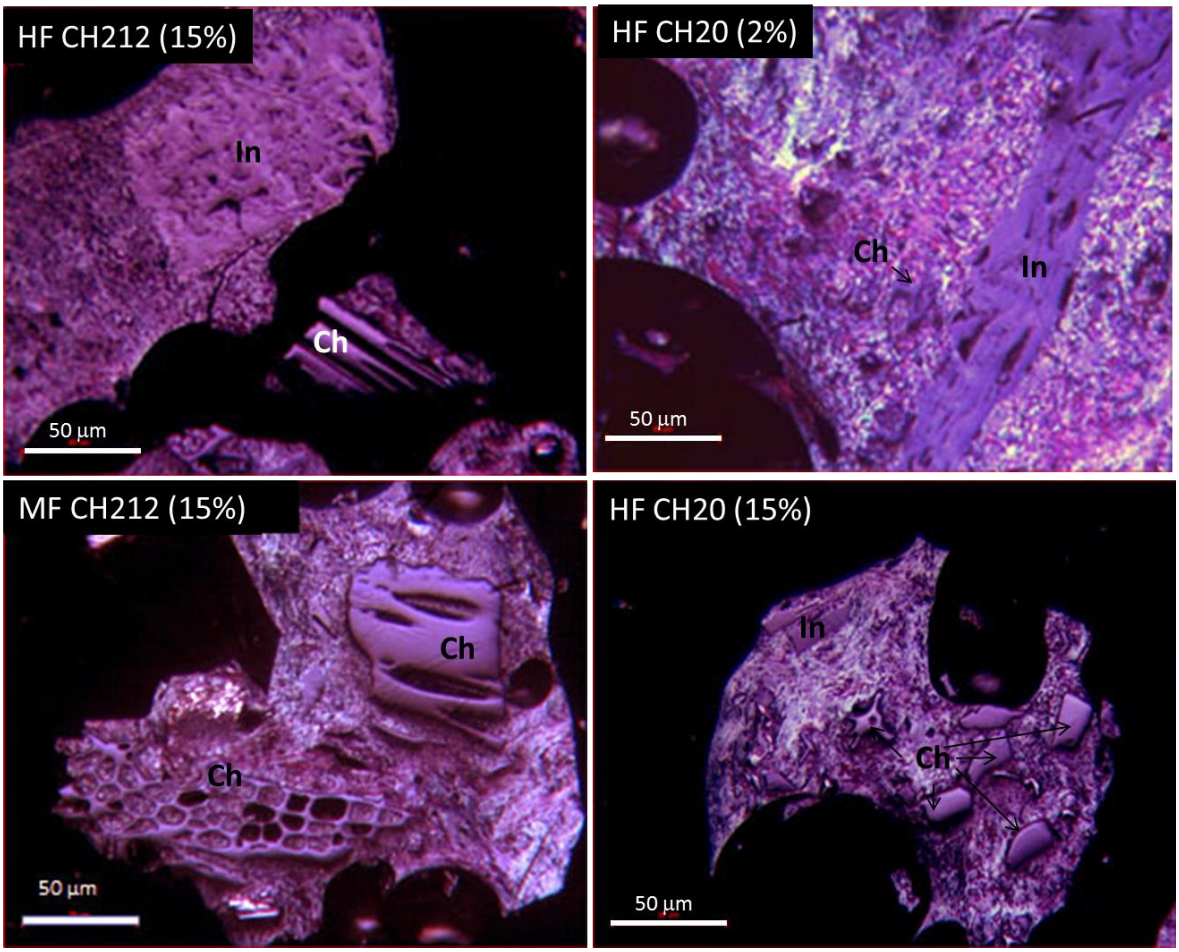

Fig.8

Figure 9

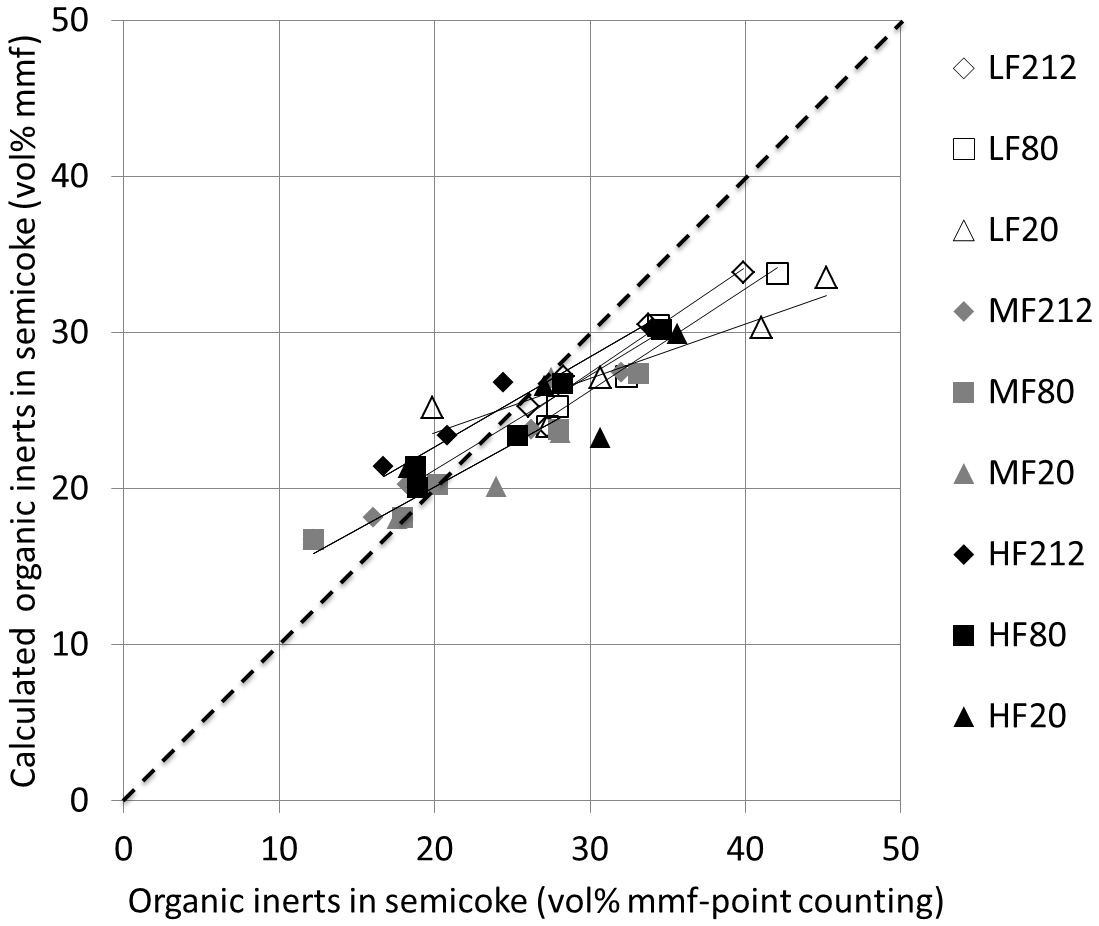

Fig.9